

Article

Autotrophic and Heterotrophic Growth Conditions Modify Biomolecule Production in the Microalga *Galdieria sulphuraria* (Cyanidiophyceae, Rhodophyta)

Roberto Barone ^{1,*}, Lorenzo De Napoli ², Luciano Mayol ², Marina Paolucci ^{3,4,*}, Maria Grazia Volpe ⁴, Luigi D'Elia ⁵, Antonino Pollio ⁵, Marco Guida ⁵, Edvige Gambino ⁵, Federica Carraturo ⁵, Roberta Marra ¹, Francesco Vinale ^{6,7}, Sheridan Lois Woo ^{2,7,*} and Matteo Lorito ^{1,7}

¹ Department of Agricultural Science, University of Naples Federico II, Via Università, Portici, 80138 Naples, Italy; robmarra@unina.it (R.M.); matteo.lorito@unina.it (M.L.)

² Department of Pharmacy, University of Naples Federico II, Via D. Montesano, 80138 Naples, Italy; lorenzo.denapoli@unina.it (L.D.N.); luciano.mayol@unina.it (L.M.)

³ Department of Science and Technologies (DST), University of Sannio, 82100 Benevento, Italy

⁴ Institute of Food Sciences, National Research Council (ISA-CNR), Via Roma 64, 83100 Avellino, Italy; mgvolpe@isa.cnr.it

⁵ Department of Biology, University of Naples Federico II, Via Cinthia, 80138 Naples, Italy; luigi.delia@unina.it (L.D.); antonino.pollio@unina.it (A.P.); .marco.guida@unina.it (M.G.); ed.gambino@gmail.com (E.G.); federica.carraturo@unina.it (F.C.)

⁶ Department of Veterinary Medicine and Animal Production, University of Naples Federico II, Via Federico Delpino, 80138 Naples, Italy; frvinale@unina.it

⁷ IPSP-CNR-Via Università-Portici, 80138 Naples, Italy

* Correspondence: robbaron@unina.it (R.B.); paolucci@unisannio.it (M.P.); woo@unina.it (S.L.W.); Tel.: +39-081-2534544 (R.B.); +39-0824-305126 (M.P.); +39-081-2539010 (S.L.W.)

Received: 26 February 2020; Accepted: 17 March 2020; Published: 18 March 2020



Abstract: Algae have multiple similarities with fungi, with both belonging to the *Thallophyte*, a polyphyletic group of non-mobile organisms grouped together on the basis of similar characteristics, but not sharing a common ancestor. The main difference between algae and fungi is noted in their metabolism. In fact, although algae have chlorophyll-bearing thalloids and are autotrophic organisms, fungi lack chlorophyll and are heterotrophic, not able to synthesize their own nutrients. However, our studies have shown that the extremophilic microalga *Galdieria sulphuraria* (GS) can also grow very well in heterotrophic conditions like fungi. This study was carried out using several approaches such as scanning electron microscope (SEM), gas chromatography/mass spectrometry (GC/MS), and infrared spectrophotometry (ATR-FTIR). Results showed that the GS, strain ACUF 064, cultured in autotrophic (AGS) and heterotrophic (HGS) conditions, produced different biomolecules. In particular, when grown in HGS, the algae (i) was 30% larger, with an increase in carbon mass that was 20% greater than AGS; (ii) produced higher quantities of stearic acid, oleic acid, monounsaturated fatty acids (MUFAs), and ergosterol; (iii) produced lower quantities of fatty acid methyl esters (FAMES) such as methyl palmytate, and methyl linoleate, saturated fatty acids (SFAs), and polyunsaturated fatty acids (PUFAs). ATR-FTIR and principal component analysis (PCA) statistical analysis confirmed that the macromolecular content of HGS was significantly different from AGS. The ability to produce different macromolecules by changing the trophic conditions may represent an interesting strategy to induce microalgae to produce different biomolecules that can find applications in several fields such as food, feed, nutraceutical, or energy production.

Keywords: *Galdieria sulphuraria*; microalga; fungi; autotrophy; heterotrophy; fatty acids; ATR-FTIR

1. Introduction

Microalgae are unicellular organisms commonly found in fresh and marine waters. They are very similar to fungi [1], both are morphologically undifferentiated and included in the group of *Thallophytes*. However, the main difference is that algae require light, contain chlorophyll, and are autotrophs. Members are characterized by a high biodiversity whose potential, in terms of the production of high value biological molecules, is yet to be explored and exploited [2]. Microalgae cultivation can provide diverse essential nutrients, including carbohydrates, proteins, and lipids, as well as pigments, vitamins, bioactive compounds, and antioxidants [3,4]; substances that can be utilized in nutraceuticals, pharmaceuticals, biofuels, health supplements, and the cosmetic industry. Furthermore, microalgae cultivation provides a potential strategy to produce an alternative food source for both humans and animals. This feature, plus the ability of microalgae to grow more rapidly than vascular plants, satisfies the need for large-scale, cost-effective, high nutritional value production [5]. Therefore, microalgae represent an interesting resource in the biotechnology field, as they are able to quickly reach a high level of biomass and produce a large quantity of fatty acids (FAs) such as palmitic acid (C16:0), myristic acid (C14:0), monounsaturated (MUFAs), polyunsaturated FAs (PUFAs), and fatty acid methyl esters (FAMES), molecules extremely interesting for commercial applications. Microalgae also produce pharmacologically active molecules with immunomodulatory, anti-inflammatory, antihypercholesterolemic, antioxidant, anticancer, and antidiabetic properties [6–8]. The metabolic flexibility of microalgae allows them to grow in both autotrophic and heterotrophic conditions [9]. The benefit trade-offs are diverse for algae, whereby the autotrophic growing condition is preferred from an efficiency point of view, but it provides a limited growth of biomass, whereas the biomass obtained under heterotrophic growing conditions is greater, but requires additional external carbon sources that are energetically expensive [10,11]. The heterotrophic cultivation of *Chlorella vulgaris*, the oldest microalgae exploited for commercial application, has demonstrated higher biomass yields than the autotrophic cultivation, with higher lipid productivity [12].

Galdieria sulphuraria (GS; Cyanidiophyceae, Rhodophyta) is an ancient extremophilic unicellular red microalga capable of growing in hot springs at low pH [13,14] all around the world. It shows optimal growth conditions at pH 1.5 and temperatures in the range of 35–45 °C, extreme growth conditions that prevent bacterial contamination, one of the major problems faced with large scale microalgae cultivation [15,16]. Moreover, GS is able to grow photoautotrophically, heterotrophically, and mixotrophically, but to date, not much is known about the morphological and biochemical changes induced by the different growing conditions or the effect on the production of different biomolecules by the microalgae. It has been noted that heterotrophic growth of GS leads to cytological changes in the cell size, probably due to reduced chloroplast size and increased number of mitochondria, the organelles directly connected with nutrition [17]. GS exhibits a high metabolic flexibility that is matched by few other microorganisms, demonstrating the ability to thrive on more than 50 different carbon sources such as sugars, sugar alcohols, tricarboxylic-acid-cycle intermediates, and amino acids [18–21]. In addition, this genus has very high daily productivity of various bioactive compounds [15] and significant potential as a source of antioxidants and macronutrients, features that have driven interest towards conduct investigations on this Cyanidiophyceae for its potential biotechnological applications [22–25]. In the present study, a comparison was made on the growth and metabolism of GS cultured under both autotrophic and heterotrophic conditions, and the different biomolecules obtained under the different growing conditions were characterized and identified by using a combination of techniques: scanning electron microscope (SEM), gas chromatography/mass spectrometry (GC/MS), and infrared spectrophotometry (ATR-FTIR). The well-known, studied, and commercialized microalgae *Spirulina platensis* (Sp) was grown in autotrophic conditions and used in this study as a comparison species. The final aim of this investigation was to verify the possibility of directing or manipulating the metabolic flexibility of GS as a tool to induce the production of biomass and biomolecules that can be of interest to several important fields such as food, feed, nutraceutical, or energy production industries.

2. Results

2.1. Scanning Electron Microscopy

An increase in the cell dimension of GS grown in heterotrophic conditions with respect to the autotrophic conditions was detected by SEM analysis. The average cell size of heterotrophic (HGS) conditions was about 30% bigger than autotrophic (AGS) conditions (Figure 1). Moreover, AGS showed different element contents with respect to the heterotrophic conditions (Figure 2).

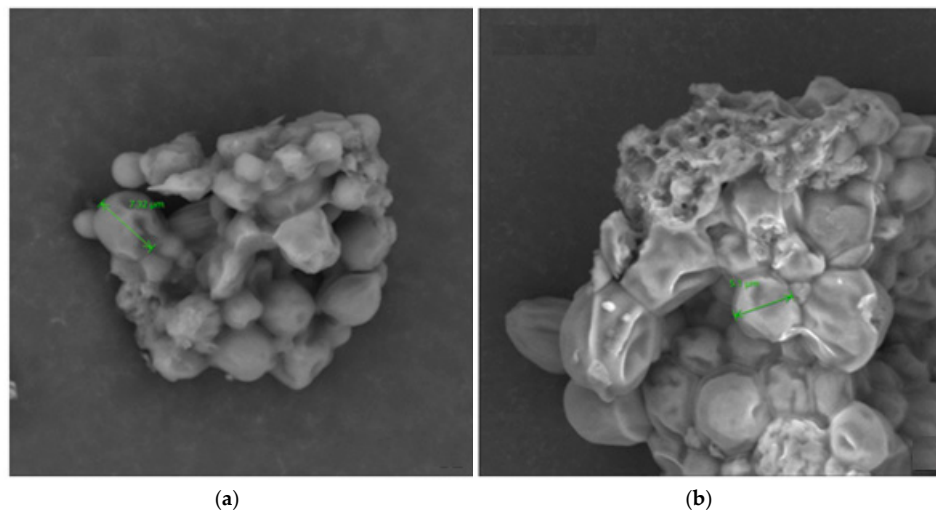


Figure 1. *Galdieria sulphuraria* strain ACUF 064 cultured in (a) heterotrophic (FOV: 62.5 μm , mode: 15kV-point, detector: BSD full) and (b) autotrophic conditions (FOV 39.5 μm , mode: 15kV-point, detector: BSD full).

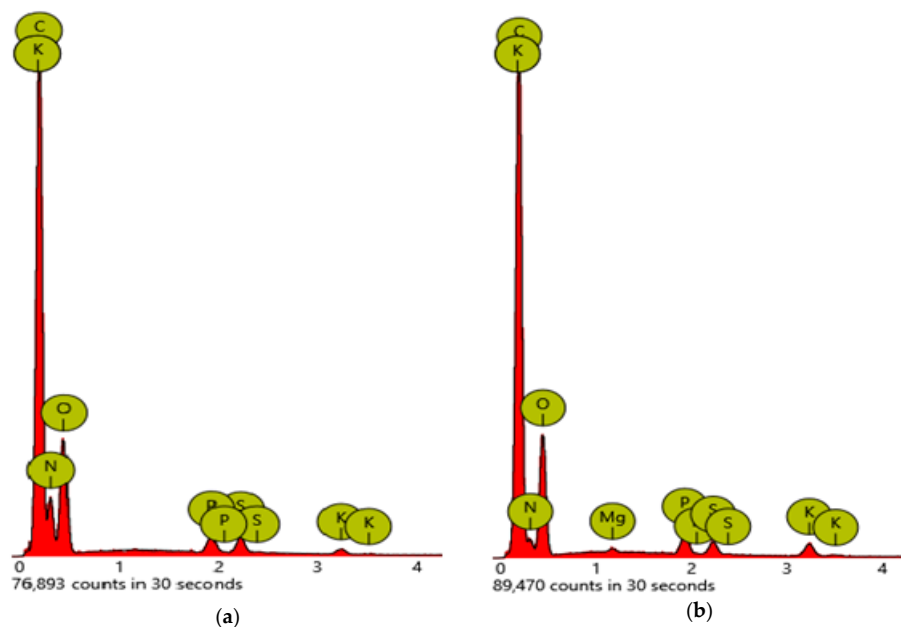


Figure 2. Different content of elements in *Galdieria sulphuraria* strain ACUF 064 cultured in heterotrophic (a) and autotrophic (b) conditions. Percentages are reported in Table 1.

Area values are reported in Table 1. A significant increase in carbon mass of 20% for the heterotrophic growth conditions was observed.

Table 1. Area values of different elements of *Galdieria sulphuraria* strain ACUF 064 cultured in autotrophic (AGS) and heterotrophic (HGS) conditions.

Element Number	Element Symbol	Element Name	Atomic Conc. HGS	Weight Conc. HGS (%)	Atomic Conc. AGS	Weight Conc. AGS (%)
6	C	Carbon	63.81	57.16	51.79	46.03
8	O	Oxygen	23.74	28.33	21.20	25.11
7	N	Nitrogen	11.40	11.90	26.40	27.37
15	P	Phosphorus	0.38	0.89	0.24	0.55
19	K	Potassium	0.32	0.93	0.11	0.31
16	S	Sulfur	0.27	0.64	0.26	0.62
12	Mg	Magnesium	0.08	0.15	0.00	0.00

2.2. GC-MS Analysis

Fatty acid (FA) composition of *Galdieria sulphuraria* strain ACUF 064 cultivated in autotrophic (AGS) and heterotrophic (HGS) conditions and *Spirulina platensis* (Sp) for comparison are reported in Table 2.

Table 2. Comparison of the fatty acid composition of *G. sulphuraria* strain ACUF 064 cultivated in autotrophic (AGS) and heterotrophic (HGS) conditions, and to *Spirulina platensis* (Sp) grown in autotrophic conditions. Values are reported as mean values ($n = 3$) \pm SD, where SD is the standard deviation.

Molecular Formula	Peak	RT (min)	Compound	AGS	HGS	Sp
C8:0	1	7.53	Caprylic acid C8:0	0.060 \pm 0.01	-	0.04 \pm 0.03
C13:0	2	10.26	Tridecanoic acid	0.35 \pm 0.01	-	0.50 \pm 0.02
C14:0	3	11.28	Myristic acid C14:0	1.74 \pm 0.14 ^a	1.90 \pm 0.12 ^a	0.13 \pm 0.01 ^b
C14:1	4	12.41	Myristoleic acid C14:1	0.10 \pm 0.03	-	0.05 \pm 0.04
C15:0	5	12.54	Pentadecanoic acid C15:0	0.61 \pm 0.09 ^a	0.36 \pm 0.09 ^a	0.03 \pm 0.01 ^b
C16:0	6	14.28	Palmitic acid C16:0	27.19 \pm 0.12 ^b	21.15 \pm 0.31 ^c	22.51 \pm 0.27 ^a
C16:1	7	15.96	Palmitoleic acid C16:1	0.32 \pm 0.09 ^b	0.33 \pm 0.16 ^b	4.74 \pm 0.41 ^a
C17:0	8	16.50	Heptadecanoic acid C17:0	0.27 \pm 0.06 ^a	0.31 \pm 0.07 ^a	0.16 \pm 0.08 ^{ab}
C17:1	9	18.62	<i>cis</i> -10-Heptadecenoic acid	0.26 \pm 0.02 ^{ab}	0.21 \pm 0.08 ^b	0.32 \pm 0.04 ^a
C18:0	10	19.43	Stearic acid	1.04 \pm 0.11 ^b	2.96 \pm 0.06 ^a	0.72 \pm 0.11 ^c
C18:1 n9t	11	21.07	Elaidic acid	0.15 \pm 0.08 ^a	0.17 \pm 0.01 ^a	0.04 \pm 0.01 ^b
C18:1 n9c	12	21.82	Oleic acid	20.91 \pm 0.14 ^b	30.07 \pm 0.16 ^a	2.95 \pm 0.09 ^c
C18:3 n3	13	24.01	Linolenic acid	5.90 \pm 0.27 ^a	3.31 \pm 0.18 ^{ab}	0.10 \pm 0.03 ^c
C18:3 n6	14	25.58	γ -Linolenic acid	-	-	13.15 \pm 0.09
C18:2 n6c	15	26.13	Linoleic acid	18.91 \pm 0.13 ^a	14.31 \pm 0.62 ^{ab}	19.06 \pm 0.51 ^a
C20:0	16	28.25	Arachidic acid	0.05 \pm 0.01	0.10 \pm 0.07	0.04 \pm 0.01
C28H44O	17	28.47	Ergosterol	-	10.21 \pm 0.13 ^a	2.93 \pm 0.21 ^b
C20H40O	18	29.75	Phytol	15.34 \pm 0.14 ^b	6.05 \pm 0.09 ^c	16.07 \pm 0.76 ^a
C15H13N	19	30.01	4'-methyl-2-phenylindole	-	7.01 \pm 0.03 ^a	2.86 \pm 0.04 ^b
C17H36	20	33.47	n-Heptadecene	5.72 \pm 0.35 ^b	-	12.92 \pm 0.47 ^a
C20:1	21	33.61	<i>cis</i> -11-Eicosenoic acid	0.26 \pm 0.11 ^b	0.53 \pm 0.02 ^a	0.01 \pm 0.01 ^c
C20:2	22	34.08	<i>cis</i> -11,14-Eicosadienoic	0.57 \pm 0.08 ^a	0.65 \pm 0.03 ^a	0.25 \pm 0.16 ^b
C20:3 n6	23	34.12	<i>cis</i> -8,11,14-Eicosatrienoic acid	-	-	0.28 \pm 0.07
C20:3 n3	24	35.03	<i>cis</i> -11,14,17-Eicosatrienoic acid	0.14 \pm 0.05	0.28 \pm 0.01	-
C24:1	25	35.97	Nervonic acid	0.11 \pm 0.02	0.09 \pm 0.01 ^{ab}	0.14 \pm 0.08 ^a
C19H34O2	N.P.A.		Methyl linoleate	0.785 \pm 0.16 ^a	3.47 \pm 0.03 ^b	-
C17H34O2			Methyl palmytate	11.41 \pm 0.73 ^a	6.21 \pm 0.03 ^b	4.01 \pm 0.62 ^b
C16H32O2			Hexadecanoic acid, methyl ester	9.47 \pm 0.49 ^a	-	6.23 \pm 0.31 ^b
Σ -FATTY ACIDS			Σ -FAME	28.73 \pm 0.74 ^a	9.68 \pm 0.03 ^b	-
			Σ -SFA	34.10 \pm 0.21 ^b	31.56 \pm 0.03 ^c	40.02 \pm 0.26 ^a
			Σ -MUFA	30.11 \pm 0.47 ^b	38.54 \pm 0.03 ^a	8.25 \pm 0.07 ^c
			Σ -PUFA	31.52 \pm 0.83 ^b	27.43 \pm 0.61 ^c	35.82 \pm 0.62 ^a

Organic compounds expressed as mean percentages of 100 mg of dry tissue weight. Values with different letters are significantly different ($p < 0.05$). N.P.A: naturally present in alga. See the Abbreviation section for the definitions of SFA, MUFA, and PUFA.

In the autotrophic conditions, higher levels of fatty acid methyl esters (FAMES) were present, especially methyl palmitate and methyl linoleate. Another compound present in higher quantities in AGS was phytol (PYT), an acyclic diterpenoid alcohol constituent of chlorophyll. The heterotrophic condition influenced the production of ergosterol, a phytosterol, stearic acid (STA) and oleic acid, present in higher concentrations with respect to the autotrophic condition. Omega 3 long chain FAs, such as EPA, DHA, and arachidonic acid, were found neither in the autotrophic nor in the heterotrophic conditions.

2.3. ATR-FTIR

Mean FTIR spectra of GS strain ACUF 064 cultivated in autotrophic (AGS) and heterotrophic (HGS) conditions and Sp are shown in Figure 3. Each spectrum is the average of three raw spectra originating from five samples.

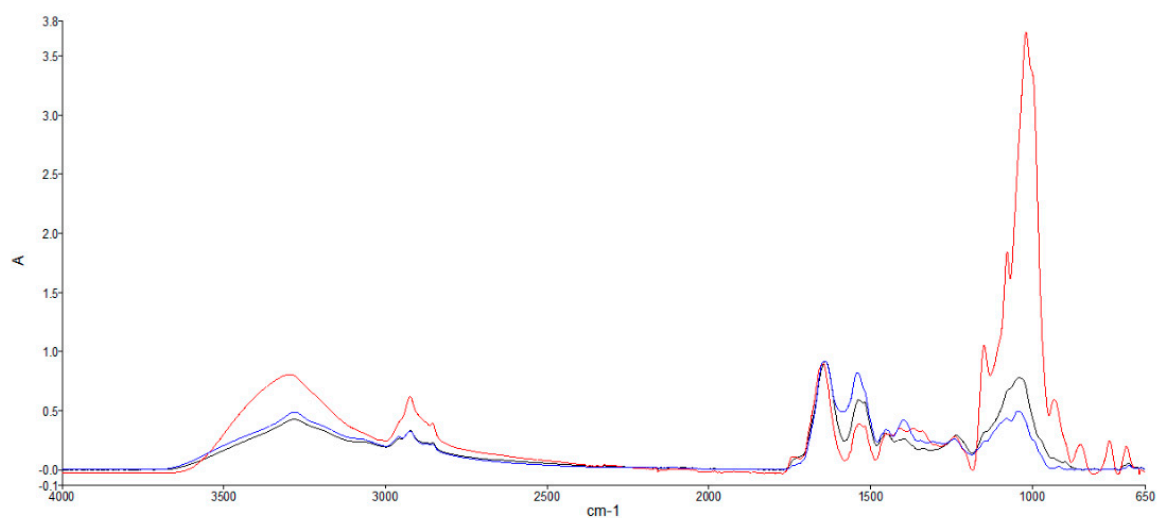


Figure 3. Infrared spectrophotometry (ATR-FTIR) spectra of *Galdieria sulphuraria* strain ACUF 064 cultured in autotrophic (—) and heterotrophic (—) conditions. (—) *Spirulina platensis*.

Each FTIR spectrum is formed by peaks arising from the infrared absorption of functional groups. The vibration intensity, reported as absorbance, is proportional to the relative abundance of organic molecules such as carbohydrates, lipids, and proteins. Table 3 reports FTIR peak assignments based on spectral values indicated in the current literature [26,27]. Although a certain degree of overlapping is present, macromolecules can be identified in relation to specific wavelength ranges [28]. Lipids can be identified in the range 3000–2800 and around 1740 cm^{-1} , proteins in the range 3600–3000 and around 1640 and 1540 cm^{-1} , and carbohydrates in the range 1174–950 cm^{-1} .

Table 3. Peak assignment of *Galdieria sulphuraria* strain ACUF 064 cultured in autotrophic (AGS) and heterotrophic (HGS) condition and *S. platensis*, based on the literature [26,27].

Spectral Ranges Analyzed with SIMCA	Peak Wavelength (cm ⁻¹)			Peak Assignment	Macromolecules
	AGS	HGS	Sp		
3600–3000		3298		ν (N-H) stretching of amide A	Proteins
	3284		3282		
2999–2800			2959	ν_{as} (CH ₂) and ν_s (CH ₂) stretching	Lipids, triglycerides, fatty acids, carbohydrates
	2924	2924	2925		
	2854	2855			
1772–1712		1743		ν (C=O) stretching of esters	Cellulose–fatty acids
1711–1576	1640	1646	1641	Amide I ν (C=O) stretching	Proteins
1575–1478	1538	1537	1541	Amide II δ (N-H) bending and ν (C-N) stretching	Proteins
1477–1175	1453	1453	1452	δ_{as} (CH ₂) and δ_{as} (CH ₃) bending of methyl	Proteins, lipids
	1394	1411	1399		
		1368		δ_s (CH ₂) and δ_s (CH ₃) bending of methyl; ν_s (C-O) of COO- groups; δ_s (N(CH ₃) ₃) bending of methyl	Proteins and lipids
	1336				
		1308	Amide III	Proteins	
	1236	1238	1240	ν_{as} (>P=O) stretching of phosphodiester	Nucleic acids and phospholipids
1174–950		1148		ν (C-O-C)	Carbohydrates (including glucose, fructose, glycogen, etc.), polysaccharides
		1077	1079		
	1039		1043		
949–650		1018		Fingerprint region	
	806	931	916		
	763	850	880		
	700	760	743		
		662			

The overlapping spectra reported in Figure 3 indicated how the intensity of the peaks corresponding to proteins, lipids, and carbohydrates was greater in HGS than in AGS and Sp, with the only exception of the peak around 1540 cm⁻¹, ascribable to N–H stretching of proteins, which was higher in Sp, followed by AGS. HGS was richer in polysaccharides and sugars compared to AGS and Sp, as indicated by the high absorbance in the range 1174–950 cm⁻¹. Polysaccharides in HGS were highlighted by the two peaks at 1148 and 1018 cm⁻¹, which were missing in AGS and Sp. Special attention should be devoted to the 950–650 cm⁻¹ region, also called the “fingerprint region”. In particular, HGS showed four different sharp absorption bands (931, 850, 760, 662 cm⁻¹) that represent a characteristic fingerprint of HGS, different from AGS and Sp that presented a very similar pattern in this region. A representative FTIR subtraction spectrum of HGS minus AGS highlights the differences in the concentration of macromolecules between autotrophic and heterotrophic conditions (Figure 4A). In order to quantify the different content of macromolecules such as lipids, carbohydrates, and proteins, the second derivative of the FTIR profiles was determined (Figure 4B).

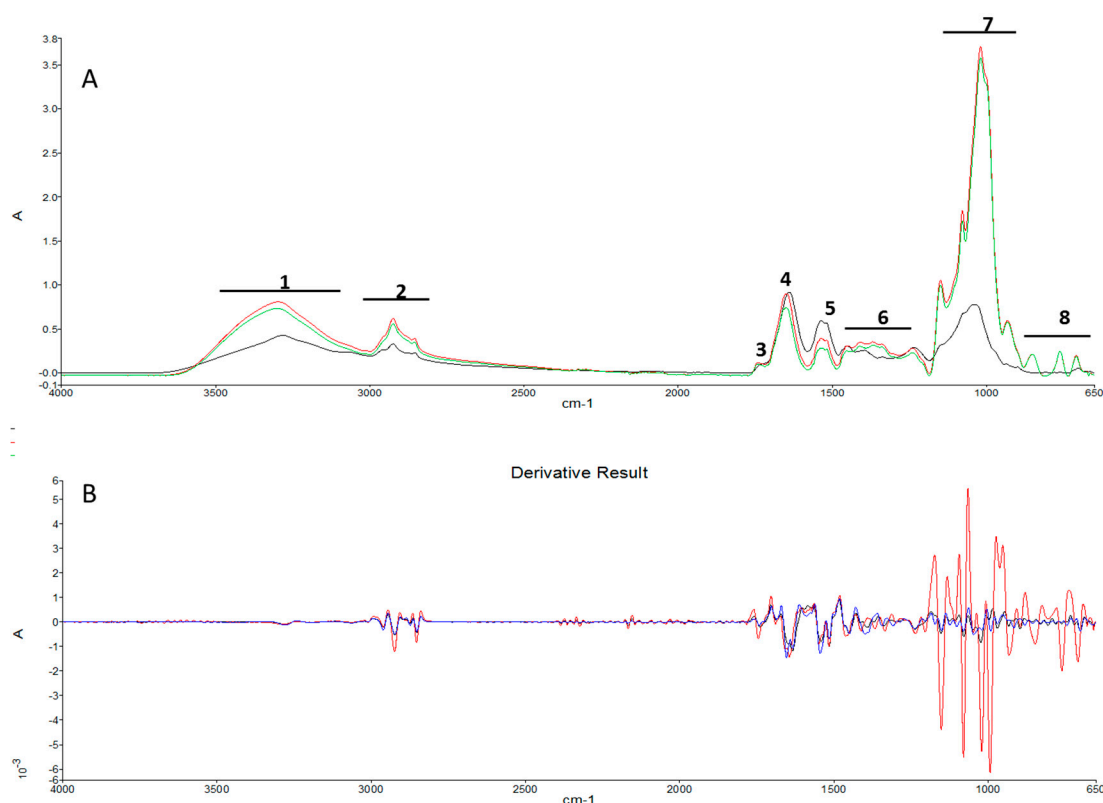


Figure 4. (A) Representative ATR-FTIR spectra of *Galdieria sulphuraria* strain ACUF 064 cultured in autotrophic (—) and heterotrophic (—) conditions and the subtraction spectrum (—). (B) Second derivatives of *Galdieria sulphuraria* strain ACUF 064 cultured in autotrophic (—) and heterotrophic (—) conditions. (—) *Spirulina platensis*.

To make a quantitative determination, the integration of the second derivative peaks was carried out according to Equation (2), reported in the Materials and Methods section. HGS compared to AGS showed a greater content of proteins, lipids, and carbohydrates of 91%, 57%, and 98%, respectively. The areas are reported in Table 4.

Table 4. Representative peak area relative to the second derivative subtraction spectrum between *Galdieria sulphuraria* grown in heterotrophic conditions and autotrophic conditions. In the first column, the FT-IR ranges are reported, as shown in Figure 4a. The subtraction area ($\Delta_{HGS-AGS}$) for each interval is expressed as the percentage of \log_{10} /total area.

<i>Spectral Ranges (cm⁻¹)</i>			
FTIR	Start	End	$\Delta_{HGS-AGS}$
1	3600	3000	2.23 (18.63%)
2	2999	2800	1.16 (9.69%)
3	1772	1712	0.20 (1.67%)
4	1711	1576	1.62 (13.53%)
5	1575	1478	1.09 (9.11%)
6	1477	1175	1.78 (14.87%)
7	1174	950	2.60 (21.72%)
8	949	650	1.29 (10.78%)

FTIR spectra of HGS, AGS, and Sp were quite complex and required a multivariate statistical analysis for the data comparison. In this study, we used a chemometric approach based on the principal component analysis to analyze the whole spectral range and sub-ranges corresponding to specific

macromolecules as reported in Table 5. Data interpretation by means of SIMCA (soft independent modeling class algorithm) algorithm (Figure 5) confirmed the differences in macromolecules between the autotrophic and heterotrophic culture conditions.

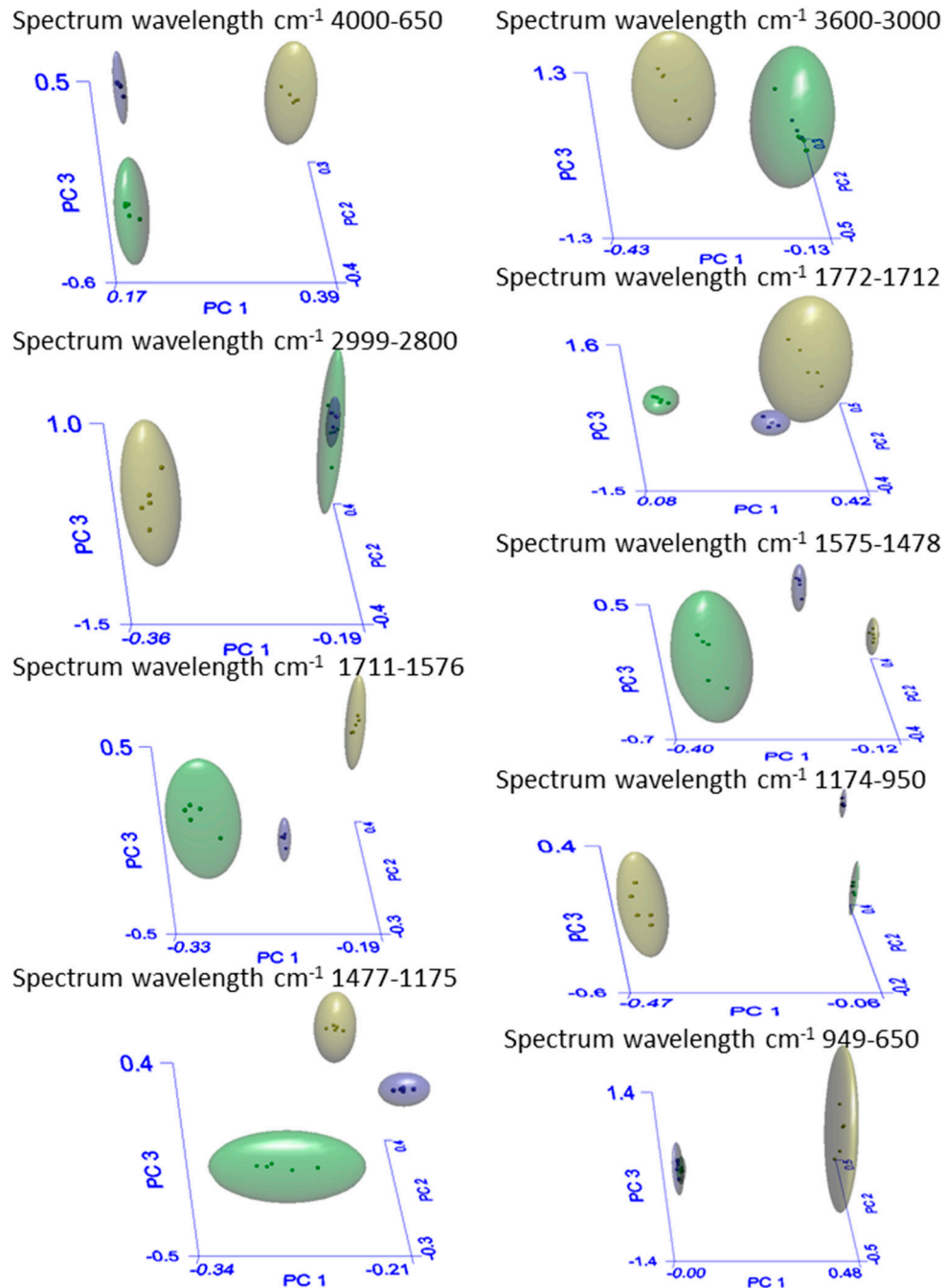


Figure 5. Three-dimensional principal component analysis score plot of *Galdieria sulphuraria* strain ACUF 064 cultivated in autotrophic (■) and heterotrophic conditions (■), plus *Spirulina platensis* in autotrophic conditions (■). Data analysis was performed in the spectrum ranges reported in the rectangles above each plot.

The significant differences between the autotrophic and the heterotrophic conditions are demonstrated by the interclass distance (ID) reported in Table 5. The ID highlights the similarities between AGS and Sp (Sp-AGS), as well as the differences between them and HGS (AGS-HGS, HGS-Sp).

The higher the ID value, the greater the difference. It is reported that a distance value higher than 3 is indicative of well separated samples, and therefore belonging to different classes [29].

Table 5. Interclass distance, and recognition and rejection rates of *Galdieria sulphuraria* strain ACUF 064 cultivated in autotrophic conditions (AGS), heterotrophic conditions (HGS), and *Spirulina platensis* (Sp).

Spectrum Wavelength cm^{-1} 4000–650				
Groups	Recognition (%) ^a	Rejection (%) ^b	Interclass Distance ^c	
AGS	100(5/5)	100(10/10)	AGS–HGS	26.2
HGS	100(5/5)	100(10/10)	HGS–Sp	36.3
Sp	100(5/5)	100(10/10)	Sp–AGS	12.2
Spectrum Wavelength cm^{-1} 3600–3000				
Groups	Recognition (%) ^a	Rejection (%) ^b	Interclass Distance ^c	
AGS	100(5/5)	100(10/10)	AGS–HGS	21.9
HGS	100(5/5)	100(10/10)	HGS–Sp	21.2
Sp	100(5/5)	100(10/10)	Sp–AGS	6.56
Spectrum Wavelength cm^{-1} 2999–2800				
Groups	Recognition (%) ^a	Rejection (%) ^b	Interclass Distance ^c	
AGS	100(5/5)	100(10/10)	AGS–HGS	24.8
HGS	100(5/5)	100(10/10)	HGS–Sp	23.9
Sp	100(5/5)	100(10/10)	Sp–AGS	4.94
Spectrum Wavelength cm^{-1} 1772–1712				
Groups	Recognition (%) ^a	Rejection (%) ^b	Interclass Distance ^c	
AGS	100(5/5)	100(10/10)	AGS–HGS	15.3
HGS	100(5/5)	100(10/10)	HGS–Sp	14.2
Sp	100(5/5)	100(10/10)	Sp–AGS	6.5
Spectrum Wavelength cm^{-1} 1711–1576				
Groups	Recognition (%) ^a	Rejection (%) ^b	Interclass Distance ^c	
AGS	100(5/5)	100(10/10)	AGS–HGS	15.4
HGS	100(5/5)	100(10/10)	HGS–Sp	36.5
Sp	100(5/5)	100(10/10)	Sp–AGS	20.8
Spectrum Wavelength cm^{-1} 1575–1478				
Groups	Recognition (%) ^a	Rejection (%) ^b	Interclass Distance ^c	
AGS	100(5/5)	100(10/10)	AGS–HGS	15.5
HGS	100(5/5)	100(10/10)	HGS–Sp	24.2
Sp	100(5/5)	100(10/10)	Sp–AGS	21.7
Spectrum Wavelength cm^{-1} 1477–1175				
Groups	Recognition (%) ^a	Rejection (%) ^b	Interclass Distance ^c	
AGS	100(5/5)	100(10/10)	AGS–HGS	22.5
HGS	100(5/5)	100(10/10)	HGS–Sp	14.7
Sp	100(5/5)	100(10/10)	Sp–AGS	17.7
Spectrum Wavelength cm^{-1} 1174–950				
Groups	Recognition (%) ^a	Rejection (%) ^b	Interclass Distance ^c	
AGS	100(5/5)	100(10/10)	AGS–HGS	78.3
HGS	100(5/5)	100(10/10)	HGS–Sp	88.2
Sp	100(5/5)	100(10/10)	Sp–AGS	13.9
Spectrum Wavelength cm^{-1} 949–650				
Groups	Recognition (%) ^a	Rejection (%) ^b	Interclass Distance ^c	
AGS	100(5/5)	100(10/10)	AGS–HGS	26.7
HGS	100(5/5)	100(10/10)	HGS–Sp	27.9
Sp	100(5/5)	100(10/10)	Sp–AGS	6.22

Notes: ^a Percentage of recognition in optimal model should be closer to 100% ; ^b percentage of rejection in optimal model should be closer to 100% ; ^c interclass distances (ID) should be as high as possible (minimum 3).

Figure 5 shows the 3D-PCA score plot generated by the SIMCA model. This multivariate analysis permits the visualization of the class separation among HGS, AGS, and Sp. The boundary ellipse (hyperboxes) defining each cluster represents a 95% confidence interval, and the points within each cluster represent the spectrum wavelengths of each sample in the three-dimensional space. Data analysis performed in smaller ranges of the spectrum (Table 5) revealed that there were significant differences among groups. The interclass distance clearly underlines the changes in GS as a consequence of the modification of the metabolism due to the growth conditions. In fact, although Sp and AGS are different microalgae species, both grown as autotrophs, they appeared to be extremely similar with an interclass distance ranging from a minimum of 4.94 (spectrum range 2999–2800 cm^{-1}) to a maximum of 21.7 (spectrum range 1575–1478 cm^{-1}), whereas HGS and AGS were found to be extremely different with a minimum inter-distance of 15.4 and a maximum of 78.3 (respectively for the intervals of 1711–1576 and 1174–950 cm^{-1}) due to the diverse metabolism imposed by the heterotrophic and autotrophic conditions.

3. Discussion

3.1. Scanning Electron Microscopy

According to the SEM analysis, the average size of GS cells grown in heterotrophic condition was about 30% greater than those cells produced in the autotrophic condition. This outcome is in agreement with Stadnichuk et al. [17] who reported an increase in the cell dimension of *Galdieria partita* grown in heterotrophic conditions with respect to the autotrophic conditions. Furthermore, the authors hypothesized that the outcome could be a result of D-glucose inhibition on the photosynthetic pigment apparatus. Interestingly, our findings noted a decrease in phytol (PYT) content, a constituent of chlorophyll, in HGS that could support this theory. Moreover, AGS exhibited different element contents with respect to the heterotrophic conditions, and there was a significant increase in carbon mass of 20% in the heterotrophic growth conditions.

3.2. GC-MS Analysis

AGS showed a different FA composition with respect to the HGS, whereby in the autotrophic conditions, higher levels of fatty acid methyl esters (FAMES) were present, especially for methyl palmitate, methyl linoleate, and hexadecanoic acid methyl ester with respect to the heterotrophic conditions. This outcome is quite interesting because it indicates the avoidance of the expensive phase of esterification that is necessary for the production of FAMES for their final application as biodiesel [30–32].

Another interesting compound present in higher quantities in AGS is phytol (PYT), an acyclic diterpenoid alcohol. Its presence is most likely related to the chlorophyll in the autotrophic form. PYT and its derivatives have a vast array of actions ranging from antimicrobial, anticancer, anti-inflammatory, and immune stimulant activities, to being a hair growth facilitator [33]. Furthermore, PYT is used as a precursor for the production of synthetic forms of vitamin E [34] and vitamin K [35], and therefore of great interest in pharmaceutical applications.

The condition of heterotrophy induced GS to produce higher levels of ergosterol, as observed in fungi [36] or phytosterol in plants, with many beneficial health effects for humans, including immunomodulatory, anti-inflammatory, neuromodulatory, antihypercholesterolemic, antioxidant, anticancer, and antidiabetic properties [37]. Ergosterol is also a biological precursor of vitamin D2 (ergocalciferol) [38], and exposure to ultraviolet light causes a photochemical reaction that activates the conversion of ergosterol to ergocalciferol. In addition, ergosterol is of great importance because it undergoes photolysis when exposed to UV light (280–320 nm) to yield provitamin D2 as one of the main products, which under thermal rearrangement, is spontaneously transformed into vitamin D2 [39]. Ergosterol and derivatives have shown a wide range of health-promoting properties, such as antioxidant, anti-inflammatory, and antihyperlipidemic activities [40]. Treatments with ergosterol

were able to significantly inhibit the proliferation of human epithelial type 2 (HEp-2) cells, a cell line originating from human laryngeal carcinoma, and the ergosterol derivatives were known to be a source of new potential antitumor or anti-angiogenesis chemotherapy agents [41]. Moreover, ergosterol derivatives have the ability to suppress lipopolysaccharide (LPS)-induced inflammatory responses of macrophages in vitro through the inhibition of highly proinflammatory cytokine (TNF- α) and cyclooxygenase-2 (COX-2) expression, as well as having a cytostatic effect on human colorectal adenocarcinoma cells [42]. Therefore, this molecule has promising multiple beneficial applications in the pharmacological field.

The heterotrophic condition was also found to influence the production of oleic acid, which was present in higher concentrations in comparison to the autotrophic condition. This is likely related to the increased cell dimensions of GS when cultured under heterotrophic conditions, and to the absence of chlorophyll a and phycocyanobilin biosynthesis, as previously observed by Stadnichuk et al. [17]. Oleic acid is a MUFA that finds interesting applications in the field of nutrition because it has the ability to reduce low density lipoprotein cholesterol (LDL-cholesterol), and at the same time, to promote high density lipoprotein cholesterol (HDL-cholesterol) [43,44]. Although the production of the omega 3 long chain FAs, such as EPA, DHA, and arachidonic acid, fundamental constituents of the human and animal diet [45], have not been found either under autotrophic or heterotrophic conditions, it is interesting to note that the autotrophic condition is accompanied by a general increase in PUFA, and in particular in linoleic and linolenic acid, which respectively belong to the omega 6 and omega 3 series. This outcome may have important consequences in the field of animal nutrition, in particular for freshwater fish nutrition, as they are able to synthesize EPA, DHA, and arachidonic acid from linoleic and linolenic acids.

The GC-MS data also indicated the presence of a high percentage of stearic acid (STA) in HGS, whereas in Sp this SFA was found to be present in negligible quantities. Recent studies have shown that stearic acid has favorable effects on human health. In fact, diets in which STA has been added in high percentages were able to drastically reduce LDL-cholesterol. STA applications may thus be of great interest in the pharmacological and nutraceutical fields [46].

3.3. Infrared Spectrophotometry

FTIR spectra of biological samples reported the macromolecular composition on the basis of the infrared absorption of functional groups [47]. The vibration intensity, reported as absorbance, is proportional to the relative abundance of organic molecules such as carbohydrates, lipids, and proteins [48]. The FTIR spectra analysis of GS provides interesting information about the changes in the macromolecule composition induced by different growth conditions, confirming the usefulness of FTIR as a fast, non-disruptive method to identify macromolecules in microalgae [49,50]. The intensity of the peaks corresponding to proteins, lipids, and carbohydrates was greater in HGS than in AGS and Sp, with the only exception with the peak observed around 1540 cm^{-1} , which was higher in Sp and AGS, and was ascribable to N-H stretching of proteins. It is worth noting that Sp had a characteristic high content of proteins, as was also reported by Rafiqul et al. [51]. HGS was richer in polysaccharides and sugars when compared to AGS and Sp., as indicated by the high absorbance in the range 1174-950 cm^{-1} . Polysaccharides in HGS are highlighted by the two peaks at 1148 and 1018 cm^{-1} , which were similar to peaks that were present in *Chlorella vulgaris* by [52], but not present in AGS and Sp.

The different contents of macromolecules such as lipids, carbohydrates, and proteins, in AGS, HGS, and Sp, was confirmed by the evaluation of the second derivative of the FTIR profiles that revealed that HGS, in comparison to AGS, had a greater content of proteins, lipids, and carbohydrates at 91%, 57%, and 98%, respectively.

The significant differences between the autotrophic and the heterotrophic conditions were also demonstrated by the interclass distance (ID), whereby the ID highlights the similarities between AGS and Sp, plus their apparent differences to HGS with the higher ID values indicating a greater difference. It has been reported that a distance value higher than 3 is indicative of well-separated samples, which

confirms their difference [53]. The interclass distance is able to underline the changes in GS as a consequence of the modification of the metabolism. Thus, metabolic changes, from autotrophic to heterotrophic, have relevant effects on both morphological and chemical characteristics of GS.

4. Materials and Methods

4.1. Strain and Growth Medium

Galdieria sulphuraria (Galdieri) Merola n. 064 was obtained from the algal collection of the Department of Biology of the University of Naples Federico II (ACUF). A preliminary screening study of 43 strains showed that the strain 064 has the lowest doubling time in autotrophic and heterotrophic conditions. Modified Allen medium [54,55] (Table 6) was used for autotrophy growth, whereas the same medium supplemented with glycerol was used for heterotrophy growth. Modified Allen medium contained NaNO_3 as a nitrogen source. The standard concentration of the nitrate was 72 g L^{-1} . H_2SO_4 was adopted for fine setting of the initial pH at 1.5. The medium was autoclaved for 20 min before use.

Table 6. Composition of modified Allen medium (pH 1.5).

Components	g/L	Oligoelements	g/L
NaNO_3	1.7	$\text{MnCl}_2 \cdot 4\text{H}_2\text{O}$	0.02
$\text{MgSO}_4 \cdot 7\text{H}_2\text{O}$	0.3	$\text{CuSO}_4 \cdot 5\text{H}_2\text{O}$	0.0001
K_2HPO_4	0.6	$\text{CoCl}_2 \cdot \text{H}_2\text{O}$	0.00005
KH_2PO_4	0.3	$\text{Na}_2\text{MoO}_4 \cdot 2\text{H}_2\text{O}$	0.00005
$\text{CaCl}_2 \cdot 2\text{H}_2\text{O}$	0.02	ZnCl_2	0.00014
NaCl	0.05	H_2SO_4	0.30
$\text{FeSO}_4 \cdot 7\text{H}_2\text{O}$	0.1		

4.2. Growth Conditions

For microalgae culture (*Galdieria sulphuraria* in autotrophic conditions (AGS), *Galdieria sulphuraria* in heterotrophic conditions (HGS), and *Spirulina platensis* (Sp), pre-cultures of 50 mL inoculated from a single isolate picked from a solid plate were grown in 200 mL Erlenmeyer flasks housed in a climatic chamber (Gibertini, Italy) at $37 \pm 1 \text{ }^\circ\text{C}$. The chamber was equipped with daylight fluorescent lamps (Philips TLD 30 W/55) set at $150 \mu\text{E/m}^2 \text{ s}$ for 24/24. After 2 weeks, the pre-cultures were used to inoculate the photobioreactors. The growth was carried out in a cylindrical bubble column photobioreactor made of glass (0.04 m ID. 0.8 m high) with a 0.9 L working volume [56]. Air was sparged at the photobioreactor bottom by means of a porous ceramic diffuser at a volumetric flow rate ranging between 20 and 200 nl h^{-1} . Filters of $0.2 \mu\text{m}$ were used to sterilize air flow inlet and outlet. The photobioreactors were housed in a climate chamber (Solar Neon) at $37 \pm 1 \text{ }^\circ\text{C}$. The chamber was also equipped with fluorescent lamps (Philips TLD 30 W/55) for autotrophic conditions. Heterotrophic cultures were conducted in the dark. In order to sustain the autotrophic growth in optimal conditions in the photobioreactor for long periods, the concentration of salts in the modified Allen culture medium was doubled with respect to that reported in Table 6. The algal biomass was harvested at the end of the exponential phase. In order to remove the biomass from the culture medium, microalgae were centrifuged at 5000 rpm for 10 min in a centrifuge JA 14. The obtained biomass was stored at $-20 \text{ }^\circ\text{C}$, and the amounts of AGS and HGS obtained were 5.20 and 4.80 g L^{-1} of wet biomass and 1.50 and 1.43 g L^{-1} of dry biomass, respectively.

4.3. Scanning Electron Microscopy

Dried samples of AGS and HGS were analyzed by scanning electron microscopy (SEM) using the ThermoFisher microscope model Phenom Pro Desktop SEM, having an electron optical magnification range: 80–150,000x; a resolution $< 10 \text{ nm}$ (BSED) and $< 8 \text{ nm}$ (SED); digital zoom: max 12x; acceleration voltages: default 5 kV, 10 kV, and 15 kV; vacuum modes: charge reduction mode (low vacuum mode)—high vacuum mode; and detector: BSD.

4.4. Lipid Extraction

The microalgal biomass was lyophilized at -86°C , using a freeze-dryer (Lyovapor L200 Buchi) according to Lee et al. [57]. Total lipids were extracted from 1.0 g of dried biomass using a mixture of chloroform/methanol (2:1 v/v) according to Bligh et al. [58]. The FAMES naturally present in the microalgae (methyl linoleate, methyl palmitate, hexadecanoic acid, methylester) were obtained. The fatty acid methyl esters naturally present in the microalgae were extracted using Soxhlet extraction, without any previous transmethylation, and were analyzed by GC-MS. The Soxhlet extraction was implemented with 2 g of sample powder on a Soxhlet system HT (Foss Soxtec 1043) for 6 h of extraction process at 140°C , using hexane as solvent, followed by 30 min solvent rinse and 30 min solvent evaporation until the exhaustion of the oil contained in the microalgae. Only after Soxhlet extraction were the total lipids transmethylated to yield their corresponding fatty acid esters (FAMES) using 2 mL of 1% NaOH in MeOH, followed by heating at 55°C for 15 min at 55°C . Next, 4.0 mL of 5% methanolic HCl were added and again heated for 15 min at 55°C [59]. Finally, total FAMES were eluted by adding 2.0 mL of *n*-hexane to the reaction mixture described above. The total FAMES obtained were readily analyzed by GC-MS in order to determine the total saturated, monounsaturated and polyunsaturated fatty acids.

4.5. GC-MS Analysis

The *n*-hexane extracts were analyzed by GC-MS on an Agilent Technologies unit mod 6850—Series II, equipped with an auto sampler G45134 and an Agilent capillary column (DB-5 type, 0.18 mm ID, film 0.18 μm , length 20 m), using the Agilent Mass Selective Detector mod 5973. Helium was used as a carrier gas at a flow rate of 13.8 mL/min. The split ratio applied was 10:1. The injector temperature was 270°C . The gradient applied was as follows: an isotherm of 2 min at 60°C , a first ramp from 60 to 250°C for 20 min ($9.5^{\circ}\text{C}/\text{min}$), followed by a second ramp from 250 to 300°C for 10 min ($10^{\circ}\text{C}/\text{min}$). The temperature was then maintained at 300°C for 5 min. All the analyses were carried out in triplicate, a confidence interval of 95% and a coverage factor $K = 2$ were applied. The limit of detection by GC-MS was 1 pmole per injection. In each case, the peak area was plotted against the standards concentration to obtain a linear relationship. As standard, a 37 component fatty acid methyl ester (FAME) mixture purchased from Supelco (37 Component FAME Mix Supelco Inc., Bellefonte, PA, USA) was used. Ergosterol (95% pure, GC assay), phytol (97% pure, GC assay), *n*-heptadecene (98% pure, GC assay), and nevrionic acid (99% pure, GC assay) were purchased from Sigma (Sigma Aldrich, St. Louis, MO, USA). All the compounds utilized were analytical grade. Serial standard dilutions with hexane were made in triplicate to obtain concentrations of 15.000, 10.000, 5.000, 2.000, 1.000, 500, 200, 100, 50, and 25 $\mu\text{g}/\text{mL}$. A 1% lauric acid methyl ester (LAME, C12:0, Sigma-Aldrich) in hexane was prepared, and LAME equivalent to 5% of the total compounds was added to each dilution as an internal standard. The standard, the sample, and the internal standard solution as the compounds determination were carried out according to Lall et al. [60]. The identification of all the compounds was carried out by the interpretations of the mass spectra, in particular the analysis of fragment ions obtained, using the Nist Mass Spectral Library Program—version 2.0 software. The peak area of standards was plotted against the standard concentration to obtain a linear relationship. In particular, the coefficient of determination r^2 values obtained from the calibration curves were in the range between 0.98 and 0.99. Values of r^2 smaller than 0.98 were not accepted. Standard curves were in the same conditions of the sample analysis previously described. In each case, the peak area was plotted against the concentration to obtain a linear relationship. Specifically, the limit of detection (LOD), limit of quantification (LOQ), and r^2 values for each peak are reported in Table 7.

Table 7. Limit of detection (LOD), limit of quantification (LOQ), and coefficient of determination (r^2).

Peak	Area			Height		
	LOD (ng/mL)	LOQ (ng/mL)	r^2	LOD (ng/mL)	LOQ (ng/mL)	r^2
1	0.21	0.63	0.9994	0.36	1.11	0.9987
2	0.19	0.57	0.9978	0.26	0.86	0.9986
3	0.30	0.90	0.9819	0.18	0.62	0.9956
4	0.14	0.42	0.9973	0.24	0.79	0.9996
5	0.15	0.46	0.9983	0.23	0.78	0.9983
6	0.19	0.58	0.9967	0.65	2.08	0.9972
7	0.20	0.61	0.9978	0.47	1.50	0.9998
8	0.33	0.97	0.9977	0.40	1.33	0.9996
9	0.22	0.68	0.9972	0.46	1.35	0.9988
10	0.19	0.59	0.9951	0.31	1.01	0.9986
11	0.14	0.43	0.9894	0.43	1.27	0.9991
12	0.16	0.47	0.9978	0.24	0.83	0.9980
13	0.21	0.63	0.9965	0.27	0.85	0.9899
14	0.23	0.69	0.9994	0.37	1.16	0.9996
15	0.18	0.56	0.9989	0.72	2.36	0.9881
16	0.16	0.48	0.9976	0.23	0.75	0.9893
17	0.22	0.70	0.9995	0.41	1.38	0.9957
18	0.21	0.63	0.9945	0.43	1.43	0.9995
19	0.24	0.73	0.9971	0.37	1.25	0.9992
20	0.27	0.81	0.9996	0.27	0.83	0.9948
21	0.21	0.64	0.9961	0.38	1.24	0.9996
22	0.25	0.76	0.9897	0.34	1.11	0.9982
23	0.18	0.54	0.9979	0.41	1.35	0.9993
24	0.17	0.50	0.9987	0.43	1.39	0.9975
25	0.19	0.59	0.9919	0.56	1.85	0.9967

4.6. ATR-FTIR Analysis

Samples of AGS, HGS, and Sp were lyophilized and analyzed without any previous treatment and placed directly on the germanium piece of the infrared spectrometer with constant pressure applied (70 ± 2 psi). The FTIR spectra were recorded in the mid-IR region ($4000\text{--}650\text{ cm}^{-1}$) at resolutions of 4 cm^{-1} with 32 scans using the Perkin Elmer FTIR Frontier coupled with DTGS (deuterated tri-glycine sulfate) detector (Perkin-Elmer Inc., Norwalk, CT, USA). Air background spectra was recorded and subtracted before analysis. To test repeatability, analyses were performed in triplicate and average spectra were used. Five samples for each group were analyzed. Spectra were baseline corrected and normalized, then elaborated using Spectrum Assure ID software, purchased with the instrument.

4.7. Statistical Analysis

The parametric test of one-way analysis of variance (ANOVA) after confirmation of normality and homogeneity of variance was used. Significant differences between experimental groups were evaluated by Duncan's multiple range test. Significant differences were determined at the 0.05 level. Data were expressed as mean \pm standard error of mean. The analyses were carried out with the Statistica version 7.0 statistical package (Statsoft Inc., Tulsa, OK, USA).

FTIR spectra were analyzed by the Spectrum AssureID software (trademark of PerkinElmer, Inc. part number 0993 4516 Release E; publication date July 2006; Software Version 4.x). Assure ID employs the SIMCA algorithm (soft independent modeling class algorithm). Three classes were defined: AGS, HGS, and Sp. For cluster analysis, the spectral ranges (I) $3600\text{--}3000$, (II) $2999\text{--}2800$, (III) $1772\text{--}1712$, (IV) $1711\text{--}1576$, (V) $1575\text{--}1478$, (VI) $1475\text{--}1175$, (VII) $1174\text{--}950$, and (VIII) $949\text{--}650\text{ cm}^{-1}$ were independently analyzed. Interclass distance between groups, recognition, and rejection rates of the samples were determined to evaluate the performance of the SIMCA model.

Second derivative was employed to obtain more specific identification of little and very close absorption peaks, which were not well-resolved in the original spectrum. According to the Beer–Lambert law, absorbance is expressed as follows:

$$A(\bar{\nu}) = \alpha(\bar{\nu})lc \quad (1)$$

where A is the wavenumber $\bar{\nu}$ -dependent absorbance, α is the wavenumber-dependent absorption coefficient, l is the optical pathlength (mainly determined by the section thickness), and c is the concentration. When Equation (1) is differentiated twice, the result is

$$\frac{d^2A(\bar{\nu})}{d\bar{\nu}^2} = \frac{d^2\alpha(\bar{\nu})}{d\bar{\nu}^2} lc \quad (2)$$

From Equation (2) it can be seen that quantitative information [61–63] can be obtained also from the second derivative spectra, as l and c are constant terms and are not affected by the differentiation.

5. Conclusions

The present study reports how it is possible to obtain different biomolecules from *G. sulphuraria* microalga by changing the culture conditions that influence the metabolic processes. This outcome expands our knowledge about the microalgae metabolism, and presents innovative strategies for developing biotechnological applications. In particular *G. sulphuraria*, due to its interchangeable and versatile metabolism, appears to be a very good candidate for the co-cultivation with fungi or other beneficial microbes for the production of bioactive molecules useful for purifying wastewater, generating biomass that represents a renewable and sustainable feedstock for biofuel, nutraceutical, pharmacological, food, or feed production [64]. Although there are still more investigations required regarding microalgae metabolic changes, our data can have significant repercussions for potential biotechnological applications in the food, animal feed, nutraceutical, pharmacological, and energy fields.

Author Contributions: M.P., S.L.W., and R.B. performed the infrared spectrophotometry experiments and edited the original draft of the manuscript; E.G., F.C., and M.G. participated in the analytical measures and in the elaboration of the data; M.G.V. performed the chemical determination by gas chromatography; L.D.N., L.M., and M.L. participated in the editing and review of the manuscript; L.D. and A.P. performed the microalgae growth in different metabolic conditions; F.V. and R.M. performed scanning electron microscopy, reviewed and edited the original draft, conceptualized the work, assisted with the data analysis, and discussed the results. All authors have read and agreed with the published version of the manuscript.

Funding: This research received no external funding.

Conflicts of Interest: The authors declare no conflict of interest.

Abbreviations: Scanning electron microscope (SEM), gas chromatography/mass spectrometry (GC/MS), infrared spectrophotometry (ATR-FTIR), fatty acids (FAs), monounsaturated fatty acids (MUFAs), fatty acid methyl esters (FAMES), polyunsaturated fatty acids (PUFAs), *Galderia sulphuraria* (GS), heterotrophic *Galderia sulphuraria* (HGS), autotrophic *Galderia sulphuraria* (AGS), *Spirulina platensis* (Sp), lipopolysaccharide (LPS), tumor necrosis factor (TNF), cyclooxygenase-2 (COX-2), eicosapentaenoic acid (EPA), docosahexaenoic acid (DHA), low density lipoprotein cholesterol (LDL), high density lipoprotein cholesterol (HDL), phytol (PYT), stearic acid (STA), lauric acid methyl ester (LAME), limit of detection (LOD), limit of quantification (LOQ), coefficient of determination (r^2).

References

1. Afonin, S.A.; Barinova, S.S.; Krassilov, V.A. A bloom of Tympanicysta Balme (green algae of zygnetatalean affinities) at the Permian-Triassic boundary. *Geodiversitas* **2001**, *23*, 481–487.
2. Sharma, N.K.; Rai, A.K. Biodiversity and biogeography of microalgae: Progress and pitfalls. *Environ. Rev.* **2011**, *19*, 1–15. [[CrossRef](#)]
3. Khan, M.I.; Shin, J.H.; Kim, J.D. The promising future of microalgae: Current status, challenges, and optimization of a sustainable and renewable industry for biofuels, feed, and other products. *Microb. Cell Fact.* **2018**, *17*, 36. [[CrossRef](#)] [[PubMed](#)]

4. de Freitas Coêlho, D.; Tundisi, L.L.; Cerqueira, K.S.; da Silva Rodrigues, J.R.; Mazzola, P.G.; Tambourgi, E.B.; de Souza, R.R. Microalgae: Cultivation Aspects and Bioactive Compounds. *Braz. Arch. Biol. Technol.* **2019**, *62*. [[CrossRef](#)]
5. Barkia, I.; Saari, N.; Schonna, R. Manning Microalgae for High-Value Products Towards Human Health and Nutrition. *Mar. Drugs* **2019**, *17*, E304. [[CrossRef](#)]
6. Ku, C.S.; Pham, T.X.; Park, Y.; Kim, B.; Shin, M.S.; Kang, I.; Lee, J. Edible blue-green algae reduce the production of pro-inflammatory cytokines by inhibiting NF- κ B pathway in macrophages and splenocytes. *BBA* **2013**, *1830*, 2981–2988. [[CrossRef](#)]
7. Pham, T.X.; Lee, Y.; Bae, M.; Hu, S.; Kang, H.; Kim, M.B.; Park, Y.K.; Lee, J.Y. Spirulina supplementation in a mouse model of diet-induced liver fibrosis reduced the pro-inflammatory response of splenocytes, reduced the pro-inflammatory response of splenocytes. *Br. J. Nutr.* **2019**, *121*, 748–755. [[CrossRef](#)] [[PubMed](#)]
8. Samuels, R.; Mani, U.V.; Iyer, U.M.; Nayak, U.S. Hypocholesterolemic effect of spirulina in patients with hyperlipidemic nephrotic syndrome. *J. Med. Food* **2002**, *5*, 91–96. [[CrossRef](#)]
9. Yang, C.; Hua, Q.; Shimizu, K. Energetics and carbon metabolism during growth of microalgal cells under photoautotrophic, mixotrophic and cyclic light-autotrophic/dark-heterotrophic conditions. *Biochem. Eng.* **2000**, *6*, 87–102. [[CrossRef](#)]
10. Kim, S.; Park, J.; Cho, Y.B.; Hwang, S.Y. Growth rate, organic carbon and nutrient removal rates of *Chlorella sorokiniana* in autotrophic, heterotrophic and mixotrophic conditions. *Bioresour. Technol.* **2013**, *144*, 8–13. [[CrossRef](#)]
11. Perez Garcia, O.; De Bashan, L.E.; Hernandez, J.P.; Bashan, Y. Efficiency of growth and nutrient uptake from wastewater by heterotrophic, autotrophic and mixotrophic cultivation of *Chlorella vulgaris* immobilized with *Azospirillum brasilense*. *J. Phycol.* **2010**, *46*, 800–812. [[CrossRef](#)]
12. Liang, Y.; Sarkany, N.; Cui, Y. Biomass and lipid productivities of *Chlorella vulgaris* under autotrophic, heterotrophic and mixotrophic growth conditions. *Biotechnol. Lett.* **2009**, *31*, 1043–1049. [[CrossRef](#)] [[PubMed](#)]
13. Yoon, H.S.; Ciniglia, C.; Wu, M.; Comeron, J.M.; Pinto, G.; Bhattacharya, D. Establishment of endolithic populations of extremophilic Cyanidiales (Rhodophyta). *BMC Evol. Biol.* **2006**, *6*, 78. [[CrossRef](#)] [[PubMed](#)]
14. Reeb, V.; Bhattacharya, D. The Thermo-Acidophilic Cyanidiophyceae (Cyanidiales). In *Red Algae in the Genomic Age, Cellular Origin, Life in Extreme Habitats and Astrobiology*; Seckbach, J., Chapman, D.J., Eds.; Springer: Dordrecht, The Netherlands, 2010; Volume 13, pp. 409–426.
15. da Silva, T.L.; Reis, A. Scale-up Problems for the Large Scale Production of Algae. In *Algal Biorefinery: An Integrated Approach*; Das, D., Ed.; Capital Publishing Company: Kolkata, West Bengal, India, 2015; pp. 125–149.
16. Graziani, G.; Schiavo, S.; Nicolai, M.A.; Buono, S.; Fogliano, V.; Pinto, G.; Pollio, A. Microalgae as human food: Chemical and nutritional characteristics of the thermo-acidophilic microalga *Galdieria sulphuraria*. *Food Funct.* **2013**, *4*, 144–152. [[CrossRef](#)]
17. Stadnichuk, I.N.; Rakhimberdieva, M.G.; Bolychevtseva, Y.V.; Yurina, N.P.; Karapetyan, N.V.; Selyakh, I.O. Inhibition by glucose of chlorophyll a and phycocyanobilin biosynthesis in the unicellular red alga *Galdieria partita* at the stage of coproporphyrinogen III formation. *Plant Sci.* **1998**, *1*, 11–23. [[CrossRef](#)]
18. Rigano, C.; Fuggi, A.; Di Martino Rigano, V.; Aliotta, G. Studies on utilization of 2-ketoglutarate, glutamate and other amino acids by the unicellular alga *Cyanidium caldarium*. *Arch. Microbiol.* **1976**, *107*, 133–138. [[CrossRef](#)]
19. Rigano, C.; Aliotta, G.; Rigano, V.D.; Fuggi, A.; Vona, V. Heterotrophic growth patterns in the unicellular alga *Cyanidium caldarium*. A possible role for threonine dehydrase. *Arch. Microbiol.* **1977**, *113*, 191–196. [[CrossRef](#)]
20. Gross, W.; Schnarrenberger, C. Purification and characterization of a galactose-1-phosphate: UDP-glucose uridylyltransferase from the red alga *Galdieria sulphuraria*. *Eur. J. Biochem.* **1995**, *234*, 258–263. [[CrossRef](#)]
21. Gross, W.; Lenze, D.; Nowitzki, U.; Weiske, J.; Schnarrenberger, C. Characterization, cloning, and evolutionary history of the chloroplast and cytosolic class I aldolases of the red alga *Galdieria sulphuraria*. *Gene* **1999**, *230*, 7–14. [[CrossRef](#)]
22. Chandra, R.; Iqbal, H.M.N.; Vishal, G.; Lee, H.S.; Nagra, S. Algal biorefinery: A sustainable approach to valorize algal-based biomass towards multiple product recovery. *Bioresour. Technol.* **2019**, *278*, 346–359. [[CrossRef](#)] [[PubMed](#)]

23. Dhivya, R.; Manimegalai, K. Preliminary Phytochemical Screening and GC- MS Profiling of Ethanolic Flower Extract of *Calotropis gigantea* Linn. (Apocynaceae). *J. Pharmacogn. Phytochem.* **2013**, *2*, 28–32.
24. Russell, E.; Lewis Pharm, D. Current Concepts in Antifungal Pharmacology. *Mayo Clin. Proc.* **2011**, *86*, 805–817.
25. Montes D'Oca, M.G.; Viégas, C.V.; Lemões, J.S.; Miyasaki, K.E.; Morón-Villarreyes, J.A.; Primel, E.G.; Abreu, P.C. Production of FAMES from several microalgal lipidic extracts and direct transesterification of the *Chlorella pyrenoidosa*. *Biomass Bioenergy* **2011**, *35*, 1533–1538. [[CrossRef](#)]
26. Movasaghi, Z.; Rehman, S.; Rehman, I. Fourier transform infrared (FTIR) spectroscopy of biological tissues. *Appl. Spectrosc. Rev.* **2008**, *43*, 134–179. [[CrossRef](#)]
27. Malek, K.; Wood, B.R.; Bambery, K.R. FTIR imaging of tissues: Techniques and methods of analysis. In *Optical Spectroscopy and Computational Methods in Biology and Medicine*; Springer: Dordrecht, The Netherlands, 2013; pp. 419–473.
28. Hirschmugl, C.J.; Bayarri, Z.E.; Bunta, M.; Holt, J.B.; Giordano, M. Analysis of the nutritional status of algae by Fourier transform infrared chemical imaging. *Infrared Phys. Technol.* **2006**, *49*, 57–63. [[CrossRef](#)]
29. He, J.; Rodriguez-Saona, L.E.; Giusti, M.M. Mid infrared spectroscopy for juice authentications rapid differentiation of commercial juices. *J. Agric. Food Chem.* **2007**, *55*, 4443–4452. [[CrossRef](#)]
30. Jun, T.D.; Chao, W.; Yubin, M.; Chen, S.Z. Two-step in situ biodiesel production from microalgae with high free fatty acid content. *Bioresour. Technol.* **2013**, *136*, 8–15.
31. Anjai, P.A.; Singh, V.B.N. Biodiesel production by esterification of free fatty acid over sulfated zirconia. *Renew. Energy* **2013**, *51*, 227–233.
32. Olivieri, G.; Marzocchella, A.; Andreozzi, R.; Pinto, G.; Pollio, A. Biodiesel production from *Stichococcus* strains at laboratory scale. *J. Chem. Technol. Biot.* **2011**, *86*, 776–783. [[CrossRef](#)]
33. Islam, M.T.; de Alencar, M.V.; da Conceição Machado, K.; da Conceição Machado, K.; de Carvalho Melo-Cavalcante, A.A.; de Sousa, D.P.; de Freitas, R.M. Phytol in a pharma-medico-stance. *Chem. Biol. Interact* **2015**, *240*, 60–73. [[CrossRef](#)]
34. Netscher, T. Synthesis of vitamin E. *Vitam. Horm.* **2007**, *76*, 155–202. [[PubMed](#)]
35. Daines, A.M.; Payne, J.R.; Humphries, M.E.; Abell, A.D. The synthesis of naturally occurring Vitamin K and Vitamin K analogues. *Curr. Org. Chem.* **2003**, *7*, 1625–1634. [[CrossRef](#)]
36. Rodrigues, M.L. The Multifunctional Fungal Ergosterol. *mBio* **2018**, *9*, e01755-18. [[CrossRef](#)] [[PubMed](#)]
37. Luo, X.; Su, P.; Zhang, W. Advances in Microalgae-Derived Phytosterols for Functional Food and Pharmaceutical Applications. *Mar. Drugs* **2015**, *13*, 4231–4254. [[CrossRef](#)] [[PubMed](#)]
38. Sankaran, M.; Isabella, S.; Amaranth, K.S. Anti proliferative Potential of Ergosterol: A Unique Plant Sterol on Hep2 Cell Line. *Int. J. Pharm. Sci. Rev. Res.* **2017**, *5*, 1736–1742.
39. Kobori, K.; Yoshida, M.; Ohnishi-Kameyama, M.; Shinmoto, H. Ergosterol peroxide from an edible mushroom suppresses inflammatory responses in RAW264.7 macrophages and growth of HT29 colon adenocarcinoma cells. *Br. J. Pharmacol.* **2007**, *150*, 209–219. [[CrossRef](#)]
40. Kim, S.K.; Ta, Q.V. Potential beneficial effects of marine algal sterols on human health. *Food Nutr. Res.* **2011**, *64*, 191–198.
41. Shimizu, T.; Kawai, J.; Ouchi, K.; Kikuchi, H.; Osima, Y.; Hidemi, R. Agarol, an ergosterol derivative from *Agaricus blazei*, induces caspase-independent apoptosis in human cancer cells. *Int J Oncol.* **2016**, *48*, 1670–1678. [[CrossRef](#)]
42. Chen, S.; Yong, T.; Zhang, Y.; Su, J.; Jiao, C.; Xie, Y. Anti-tumor and anti-angiogenic Ergosterols from *Ganoderma lucidum*. *Front. Chem.* **2017**, *5*, 85. [[CrossRef](#)]
43. Allman-Farinelli, M.A.; Gomes, K.; Favaloro, E.J.; Petocz, P.A. Diet rich in high-oleic-acid sunflower oil favorably alters low-density lipoprotein cholesterol, triglycerides, and factor VII coagulant activity. *J. Am. Diet Assoc.* **2005**, *105*, 1071–1079. [[CrossRef](#)]
44. Saini, R.K.; Keum, Y.S. Omega-3 and omega-6 polyunsaturated fatty acids: Dietary sources, metabolism, and significance. A review. *Life Sci.* **2018**, *203*, 255–267. [[CrossRef](#)] [[PubMed](#)]
45. Tocher, D.R. Metabolism and Functions of Lipids and Fatty Acids in Teleost Fish. *Rev. Fish. Sci.* **2003**, *11*, 107–184. [[CrossRef](#)]
46. Hunter, J.E.; Zhang, J.; Kris-Etherton, P.M. Cardiovascular disease risk of dietary stearic acid compared with trans, other saturated, and unsaturated fatty acids: A systematic review. *Am. J. Clin. Nutr.* **2009**, *91*, 46–63. [[CrossRef](#)]

47. Baker, M.J.; Trevisan, J.; Bassan, P.; Bhargava, R.; Butler, H.J.; Dorling, K.M.; Fielden, P.M.; Fogarty, S.W.; Fullwood, N.J.; Heys, K.A.; et al. Using Fourier transform IR spectroscopy to analyze biological materials. *Nat. Protoc.* **2014**, *9*, 1771–1791. [[CrossRef](#)] [[PubMed](#)]
48. Corte, L.; Tiecco, M.; Roscini, L.; Germani, R.; Cardinali, G. FTIR analysis of the metabolomic stress response induced by N-alkyltropylium bromide surfactants in the yeasts *Saccharomyces cerevisiae* and *Candida albicans*. *Colloid. Surf. B Biointerfaces* **2014**, *116*, 761–771. [[CrossRef](#)]
49. Mayers, J.J.; Flynn, K.J.; Shields, R.J. Rapid determination of bulk microalgal biochemical composition by Fourier-Transform Infrared spectroscopy. *Bioresour. Technol.* **2013**, *148*, 215–220. [[CrossRef](#)]
50. Bartosova, A.; Blinova, L.; Gerulova, K. Characterisation of Polysaccharides and Lipids from Selected Green Algae Species by FTIR-ATR Spectroscopy. *Fac. Mater. Sci. Technol. Trnava Slovak Univ. Technol. Bratisl.* **2015**, *23*, 97–102. [[CrossRef](#)]
51. Rafiqul, I.M.; Jalal, K.C.A.; Alam, M.Z. Environmental Factors for Optimisation of Spirulina Biomass in Laboratory Culture. *Biotechnology* **2005**, *4*, 19–22.
52. Duygu, D. Fourier transform infrared (FTIR) spectroscopy for identification of *Chlorella vulgaris* Beijerinck 1890 and *Scenedesmus obliquus* (Turpin) Kützing 1833. *Afr. J. Biotechnol.* **2012**, *11*, 3817–3824.
53. Koo, T.K.; Da, P.; Li, M.Y. A Guideline of Selecting and Reporting Intraclass Correlation Coefficients for Reliability Research. *J. Chiropr. Med.* **2016**, *15*, 155–163. [[CrossRef](#)]
54. Allen, M.M.; Stanier, R.Y. Growth division of some unicellular blue-green algae. *J. Gen. Microbiol.* **1968**, *51*, 199–202. [[CrossRef](#)] [[PubMed](#)]
55. De Luca, P.; Taddei, R. Crescita comparata di due forme di *Cyanidium caldarium* dei Campi Flegrei (Napoli) in presenza di diverse fonti di azoto. *Delpinoa* **1972**, *12*, 3–8.
56. Wang, S.K.; Stiles, A.R.; Guo, C.; Liu, C.Z. Microalgae cultivation in photobioreactors: An overview of light characteristics. *Eng. Life Sci.* **2014**, *14*, 550–559. [[CrossRef](#)]
57. Lee, J.Y.; Yoo, C.; Jun, S.Y.; Ahn, C.Y.; Oh, H.M. Comparison of several methods for effective lipid extraction from microalgae. *Bioresour. Technol.* **2010**, *101*, S75–S77. [[CrossRef](#)]
58. Bligh, E.G.; Dyer, W.J. A rapid method of total lipid extraction and purification. *Can. J. Biochem. Physiol.* **1959**, *37*, 911–917. [[CrossRef](#)]
59. Carreau, J.P.; Dubacq, J.P. Adaptation of a macro-scale method to the micro-scale for fatty acid methyl transesterification of biological lipid extracts. *J. Chromatogr. A* **1978**, *151*, 384–390. [[CrossRef](#)]
60. Lall, R.K.; Proctor, A.; Jain, V.P. A rapid, micro FAME preparation method for vegetable oil fatty acid analysis by gas chromatography. *J. Am. Oil Chem. Soc.* **2009**, *86*, 309–314. [[CrossRef](#)]
61. Rieppo, L.; Saarakkala, S.; Närhi, T.; Helminen, H.J.; Jurvelin, J.S.; Rieppo, J. Application of second derivative spectroscopy for increasing molecular specificity of fourier transform infrared spectroscopic imaging of articular cartilage. *Osteoarthr. Cartil.* **2012**, *20*, 451–459. [[CrossRef](#)]
62. Mach, H.; Thomson, J.A.; Middaugh, C.R. Quantitative analysis of protein mixtures by second derivative absorption spectroscopy. *Anal. Biochem.* **1989**, *181*, 79–85. [[CrossRef](#)]
63. Baldassarre, M.; Li, C.; Eremina, N.; Goormaghtigh, E.; Barth, A. Simultaneous Fitting of Absorption Spectra and Their Second Derivatives for an Improved Analysis of Protein Infrared Spectra. *Molecules* **2015**, *20*, 12599–12622. [[CrossRef](#)]
64. Wrede, D.; Taha, M.; Miranda, A.F.; Kadali, K.; Stevenson, T.; Ball, A.S.; Mouradov, A. Co-Cultivation of Fungal and Microalgal Cells as an Efficient System for Harvesting Microalgal Cells, Lipid Production and Wastewater Treatment. *PLoS ONE* **2014**, *9*, e113497. [[CrossRef](#)] [[PubMed](#)]

